



## Adsorption and Vibrational Study of Folic Acid on Gold Nanopillar Structures Using Surface-enhanced Raman Scattering Spectroscopy

Castillo, John J.; Rindzevicius, Tomas; Rozo, Ciro E.; Boisen, Anja

*Published in:*  
Nanomaterials and Nanotechnology

*Link to article, DOI:*  
[10.5772/61606](https://doi.org/10.5772/61606)

*Publication date:*  
2015

*Document Version*  
Publisher's PDF, also known as Version of record

[Link back to DTU Orbit](#)

*Citation (APA):*  
Castillo, J. J., Rindzevicius, T., Rozo, C. E., & Boisen, A. (2015). Adsorption and Vibrational Study of Folic Acid on Gold Nanopillar Structures Using Surface-enhanced Raman Scattering Spectroscopy. *Nanomaterials and Nanotechnology*, 5. <https://doi.org/10.5772/61606>

---

### General rights

Copyright and moral rights for the publications made accessible in the public portal are retained by the authors and/or other copyright owners and it is a condition of accessing publications that users recognise and abide by the legal requirements associated with these rights.

- Users may download and print one copy of any publication from the public portal for the purpose of private study or research.
- You may not further distribute the material or use it for any profit-making activity or commercial gain
- You may freely distribute the URL identifying the publication in the public portal

If you believe that this document breaches copyright please contact us providing details, and we will remove access to the work immediately and investigate your claim.

# Adsorption and Vibrational Study of Folic Acid on Gold Nanopillar Structures Using Surface-enhanced Raman Scattering Spectroscopy

Regular Paper

John J. Castillo<sup>1,2\*</sup>, Tomas Rindzevicius<sup>2</sup>, Ciro E. Rozo<sup>3</sup> and Anja Boisen<sup>2</sup>

1 Grupo de Investigación en Bioquímica y Microbiología, GIBIM, Universidad Industrial de Santander, Bucaramanga, Colombia

2 Department of Micro- and Nanotechnology, Technical University of Denmark, Lyngby, Denmark

3 Grupo de Investigaciones Ambientales para el Desarrollo Sostenible, Facultad de Química Ambiental, Universidad Santo Tomas, Floridablanca, Colombia

\*Corresponding author(s) E-mail: jcasleon@uis.edu.co

Received 20 March 2015; Accepted 23 September 2015

DOI: 10.5772/61606

© 2015 Author(s). Licensee InTech. This is an open access article distributed under the terms of the Creative Commons Attribution License (<http://creativecommons.org/licenses/by/3.0>), which permits unrestricted use, distribution, and reproduction in any medium, provided the original work is properly cited.

## Abstract

This paper presents a study of adsorption and vibrational features of folic acid, using surface-enhanced Raman scattering (SERS). A gold-capped silicon nanopillar (Au NP) with a height of 600 nm and a width of 120 nm was utilized to study the vibrational features of FA molecules adsorbed on the nanopillars within the high electromagnetic field areas. The adsorption behaviour of folic acid and the band assignment of the main vibrations together with the optimized geometry of folic acid and folic acid in the presence of a cluster of 10 gold atoms were assessed using the density functional theory (B3LYP(6-31G(d))) and the scalar relativistic effective core potential with a double-zeta basis set (LANL2DZ). The vibrations obtained from the solid-state folic acid and the folic acid on a gold cluster were in accordance with those observed experimentally. The analysis of the main vibrations indicated that the interaction of folic acid with the Au NP occurred primarily through the nitrogen atoms, from their pteridine ring. Finally, the obtained adsorption isotherm for folic acid was

deduced from the analysis of the SERS spectra and it followed a negative cooperative binding model.

**Keywords** Gold Nanopillars, SERS, Folic Acid

## 1. Introduction

Folic acid (FA), also known as vitamin B, is a compound of low molecular weight (441 g/mol), which is formed by a pteridine ring, p-aminobenzoic acid and glutamic acid. One of the most important biochemical functions of FA is related to its role in the folate-requiring reactions for pyrimidine and purine synthesis, as well as methylation reactions for the fabrication of DNA [1]. Since the early 1990s it has been known that there is a relationship between FA deficiency and an increased risk of birth defects and chronic diseases, as well as congenital heart defects [2]. FA is a high-affinity ligand for the folate receptor (FR) ( $K_d=1\text{nM}$ ), which maintains its strong binding properties

when conjugated to other molecules [3]. As a result, FA coupled to FR has been successfully applied in the therapy and diagnosis of cancer and tropical diseases [1]. Different methods have been developed for FA and FR detection, including cytological testing, fluorescent imaging, electrochemical methods and radio-labelled assays [4]. While the effectiveness of these methods has yet to be challenged, certain issues — like the time-consuming nature of radio-labelled assays — have encouraged us to explore new methods and techniques for FA detection.

Raman spectroscopy is a high-resolution photonic technique that provides chemical and structural information in a relatively short amount of time. Small sample areas or volumes can be used and water solution does not interfere with the spectrum. The most important disadvantage associated with the technique is perhaps the poor sensitivity that arises from the tiny amount of Raman-scattered photons, compared to those that are Rayleigh-scattered. Further disadvantages include the fluorescence displayed by samples in the spectrum and the use of laser irradiation, which in principle can damage the sample. Sensitivity issues were overcome with the development of the surface-enhanced Raman scattering (SERS) technique. The information obtained from SERS spectra contains greater detail and a higher signal than from conventional Raman spectroscopy. SERS has been widely used to obtain information for vibrational analysis and to observe the adsorption of biomolecules on metal substrates. Recent developments in the synthesis and fabrication of new colloid metal nanoparticles and solid support-based SERS substrates have led to the detection at trace levels of different compounds [5]. SERS metal substrates can be divided into two groups: i) colloid metal nanoparticles, and ii) roughened metallic surfaces [6]. The main limitation in using colloid metal nanoparticles is the formation of nanoparticle conglomerates after the addition of the sample, which often leads to poor reproducibility in the SERS spectra [7]. An ideal SERS substrate must have enough hot spots to guarantee an effective interaction with the analyte, and a homogeneous surface to produce reproducible Raman spectra. Recently, we have developed a simple method to produce flexible free-standing Au NPs for SERS applications [8]. These Au NPs produce a remarkably large enhancement of the Raman scattering signal. Yang et al. [9] have used the same Au NP as a probe in a bioassay for the specific detection of vasopressin. Surface homogeneity and reproducibility in the Raman spectra converted Au NP into a potential SERS substrates for detection and studies of the adsorption behaviour of different biomolecules.

The adsorption study of biomolecules on SERS substrates is important for the analysis, identification and quantification of these compounds [10]. Jing et al. [11] have investigated the adsorption behaviour of L-cysteine on the surface of a variety of metals. The vibrational features of adenine-containing microRNA chains adsorbed on roughened gold substrates were studied using SERS [12]. A new gold grass-

like nanostructure was used for studying the adsorption of DNA bases on polyvinyl alcohol [13]. To date, every research group has used gold-capped nanopillars for studying the adsorption behaviour of biomolecules.

Several SERS studies have been carried out to detect FA and cells over-expressing folate receptors. Boca-Farcu [14] has used SERS-labelled gold nanotriangles for the multimodal detection of human ovarian cancer cells. Hu et al. developed a cancer diagnostic probe based on reduced graphene oxide and gold nanoparticles, for the detection of FA [15]. In a very interesting work, Kokaislová et al. studied the effect of temperature on the spectral features of FA, using gold and silver SERS substrates [16]. Previous work has focused on SERS studies as a means of detecting FA and there is currently little knowledge about the adsorption and vibrational features of FA on SERS nanostructured gold substrates.

In this work, we present for the first time an adsorption SERS study for the vibrational study of FA on large-area gold-capped silicon nanopillars. The DFT methods have allowed us to calculate the Raman vibrations of FA, helping us to understand better the adsorption of FA on gold-capped nanopillars. Most of the calculated Raman vibrations coincided well with those from experimental SERS spectra. Finally, the adsorption isotherm was fitted to a Hill model exhibiting a negative cooperative binding of FA molecules on the surface of the Au NP.

## 2. Experimental Set-up

### 2.1 Measurement Tools and Techniques

Raman scattering and SERS measurements were performed using a Thermo Scientific DXR Raman microscope. An optical microscope was coupled to a single grating spectrometer with  $5\text{ cm}^{-1}$  FWHM spectral resolution and  $\pm 2$  wavenumber accuracy. A frequency-stabilized single diode laser was operated at 532 nm.

The Raman scattering spectrum of FA was collected using a 10x long working distance objective, 20 mW laser power and 5s signal accumulation times. FA SERS spectra were recorded using a 10x long working distance objective, 0.1 mW laser power and 5s signal accumulation times. The power density was kept  $\sim 12\text{ kW/cm}^2$  at the sample to minimize photoinduced and thermal effects [8].

In order to characterize the formation of FA layers adsorbed on the Au NPs, scanning electron microscopy (SEM) analysis was performed using a Quanta FEG SEM (Oregon, USA).

### 2.2 Fabrication of SERS-active Au NP Substrates

The substrates were fabricated using a three-step process. First, maskless Si RIE (reactive ion etching) was utilized to form Si NP structures. Second, an  $\text{O}_2$ -plasma process was systematically applied, in order to (i) remove Si RIE

byproducts from the Si surface, and (ii) control the Au NP cluster size. Lastly, an Au metal film was deposited on the Si NPs using e-beam evaporation. As a result, a series of vertical free-standing gold-capped silicon nanopillar structures (Au NP), surrounded by a continuous gold film at the base of the pillars, was obtained (see Fig. 1) [8]. The obtained Si NP density was approximately  $\sim 18$  pillars/ $\mu\text{m}^2$ . The Si NP dimensions were as follows: Si NP height  $\sim 600$  nm, Si NP width  $\sim 50$  nm, Au cap height and width  $\sim 300$  and  $120$  nm, respectively. All fabricated Au NP structures were utilized within three days to minimize any effects related to oxidation of the Au surface.

### 2.3 Preparation of FA Solutions

FA was obtained from Sigma-Aldrich Corp. All chemicals used in this study were of analytical grade. FA solutions were prepared as described by Castillo et al. [17]. FA molecules were dissolved in water with an addition of  $50\ \mu\text{L}$  of NaOH ( $1\ \text{M}$ ), due to the poor solubility of FA. The FA powder ( $0.029\ \text{g}$ ) was mixed with  $\text{H}_2\text{O}$  ( $25\ \text{mL}$ ) and magnetically stirred until a yellow-to-clear transition was observed.

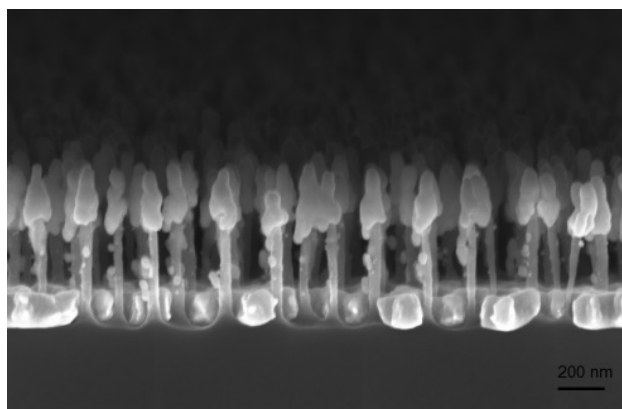


**Figure 1.** SEM image of gold-capped silicon nanopillars

### 2.4 FA Isotherms

Serial dilutions of the FA solutions in the range of  $0.1$ – $100\ \mu\text{M}$  were prepared. Single droplets ( $\sim 1\ \mu\text{L}$ ) of various FA concentrations were then dispersed on the SERS active substrates and left to dry. The droplets were then allowed to spread over the whole Au NP surface area ( $5 \times 5\ \text{mm}^2$ ) for several minutes, to ensure homogeneity in the surface coverage and to achieve a suitable time of adsorption equilibrium, and thus avoid any change due to the desorption of FA. Before every SERS measurement, the FA-Au NP was gently rinsed with Milli-Q water and dried with nitrogen flow to remove the non-adsorbed FA. The Raman scattering signal was recorded over an area of  $\sim 0.05\ \text{mm}^2$ , with  $17\ \mu\text{m}$  and  $11\ \mu\text{m}$   $x$  and  $y$  step sizes, respectively.

For each concentration, an exposure time of  $5\ \text{s/spectra}$  was used and  $238$  spectra were obtained. The  $689\ \text{cm}^{-1}$  peak

intensity averaged from the  $238$  spectra was used for the construction of the isotherm plot.

### 2.5 Computational Methods

In order to identify the main vibrations of FA Raman scattering spectra, their vibrational frequencies were calculated using the density functional theory (DFT) method, using B3LYP theory combined with the standard 6-31G(d) basis set. In order to correct for systematic errors, all calculated frequencies were scaled by a factor of  $0.9614$ , in accordance with the results reported in [18]. A cluster of Au atoms was chosen as a model system for the Au NP structures [19, 20]. In order to decrease the high computational demands for larger clusters, a cluster of  $10$  Au atoms (Au<sub>10</sub>) was selected and proven to be a good candidate for simulating the FA-Au SERS spectrum. The Au<sub>10</sub> cluster was planar and large enough to cover a representative part of the FA (see Figure 4). The interaction between the FA and Au<sub>10</sub>, the FA-Au<sub>10</sub> geometry optimization and the Raman spectra were computed using the scalar relativistic effective core potential (ECP) with double-zeta basis sets (LANL2DZ) [21]. All the geometries of the model system were fully optimized. In addition, the HOMO-LUMO energy gap and the chemical hardness [22] of the FA molecule were also calculated (see supporting information and Figure S1). The calculations were carried out using the Gaussian 09 software package [19].

## 3. Results and Discussion

### 3.1 Raman Spectra of Folic Acid

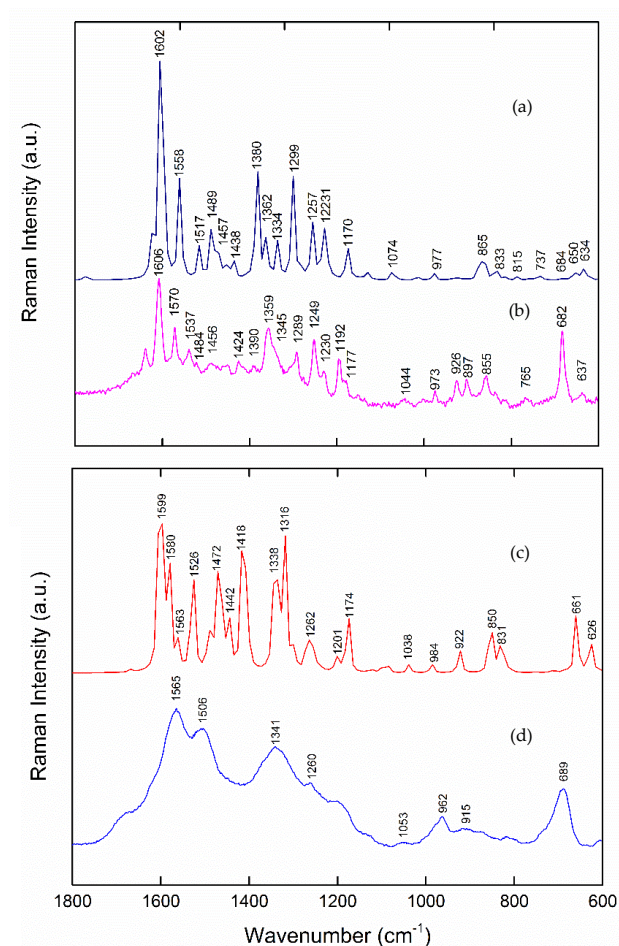
To study the vibrational frequencies and amplitudes of state solid FA, a DFT-RB3LYP(6-31G(d)) basis set was used to calculate its Raman spectra.

Table 1 and Figure 2 show the calculated and experimental Raman spectra of solid-state FA and FA adsorbed on gold-capped silicon nanopillars, respectively. Most of the vibrational bands from the solid-state FA are in good concordance with previous similar works [16]. The Raman spectra in Figure 2(b) show vibration bands mainly in the range between  $1700$  and  $600\ \text{cm}^{-1}$ . The most intense band was located at  $1606\ \text{cm}^{-1}$  and can be related to the stretching vibration of NH from the pteridine ring (pt) of the FA. Medium-strong-intensity Raman bands were vibrating at  $1570$ ,  $1359$ ,  $1249$  and  $682\ \text{cm}^{-1}$ . According to our theoretical assignment (Fig. 2a and Table 1), these observed bands are dominated by the asymmetric vibration of the C=N from the pt, the rocking vibration of the CH from the p-amino-benzoic acid moiety (paba), the rocking vibration of the C=N from the pt, and the asymmetric vibration of the C=C from paba, respectively.

The experimental and theoretical Raman vibrations were in good agreement, as is shown in Figures 2(a) and 2(b). Some of the relative positions of the Raman peaks do not correspond well with certain bands, despite the fact that



we corrected the calculated frequencies by a factor of 0.9614. However, the computational calculations were helpful for the assignment of the Raman modes of the FA in the experimental spectrum. Thus, the most intense bands present in the calculated FA Raman spectrum are also present in its experimental spectrum.



**Figure 2.** DFT-calculated (a) and experimental (b) Raman spectra of solid-state FA; DFT calculated (c) and experimental (d) SERS spectra of FA adsorbed on gold-capped silicon nanopillars

### 3.2 SERS Spectra of Folic Acid

The calculated and experimental SERS spectra of FA on gold-capped silicon nanopillars are shown in Figures 2(c) and 2(d), respectively. Figures 3(a) and 3(b) show a comparison between the calculated main vibrations of solid-state FA and FA in the presence of an Au<sub>10</sub> cluster, respectively.

The presence of new Raman bands, as well as the shifting of the main vibrations and increasing of the signal intensity, clearly indicates the effect of gold on the geometry and orientation of the FA. For example, the vibrations at 1338, 1174, 964 and 661 cm<sup>-1</sup> are Raman modes that are producing by the enhancement of the electromagnetic field, caused by the FA molecules located close to the metal silicon nanopillars. A similar Raman spectrum is obtained when FA is

Free FA (cm <sup>-1</sup> )		FA-Au NP (cm <sup>-1</sup> )		Assignment
Calc.	Exp.	Calc.	Exp.	
1602	1606	1599	1565	$s(\text{NH}_2)+v_{\text{as}}(\text{C}=\text{N})(\text{pt}); v_{\text{s}}(\text{C}=\text{C})+q(\text{CH})(\text{paba})$
1558	1570	1580	1506	$s(\text{NH}_2)+v_{\text{as}}(\text{C}=\text{N})(\text{pt})+q(\text{CH}); v_{\text{s}}(\text{C}=\text{C})+q(\text{NH})(\text{paba})$
1489	1484			$q(\text{NH})(\text{OH})+v_{\text{s}}(\text{C}=\text{C})(\text{GA})$
1334				$\omega(\text{CH}_2)(\text{paba}); q(\text{CH})(\text{OH})(\text{GA})$
1257	1249			$q(\text{NH})(\text{OH})+\omega(\text{CH}_2)(\text{GA})$
1231	1230			$q(\text{NH})(\text{OH})+\omega(\text{CH}_2)(\text{GA})$
1074	1044	1038		$q(\text{NH})(\text{OH})+\omega(\text{CH}_2)(\text{GA})$
977	973	984	962	$q(\text{CH}_2)(\text{paba})$
650	682	661	689	$v_{\text{s}}(\text{C}=\text{N})(\text{pt}); v_{\text{as}}(\text{C}=\text{C})(\text{paba})$

<sup>a</sup>symbols: v, stretching;  $\delta$ , bending; q, rocking;  $\omega$ , wagging; s, scissoring; ar, aromatic; GA, glutamic acid; pt, pteridine; paba, p-aminobenzoic acid

**Table 1.** Assignment of the experimental and calculated Raman and SERS bands of free FA and FA adsorbed on Au NPs

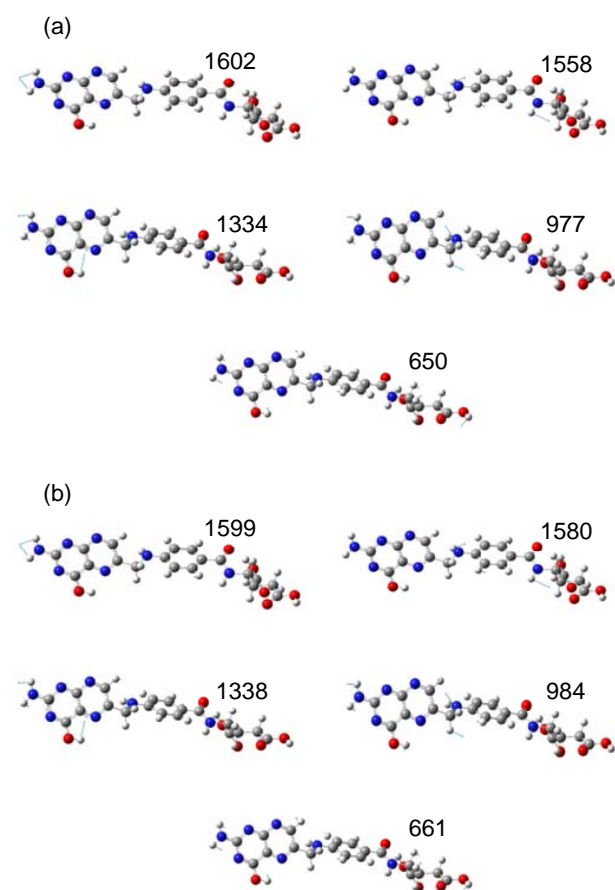


**Figure 3.** Comparison of the calculated main vibrations (cm<sup>-1</sup>) for the theoretical Raman-active solid-state FA and FA-Au<sub>10</sub> modes, (a) and (b) respectively

adsorbed on the surface of gold-silicon nanopillars (Fig. 2(d)). Most of the SERS vibrations of FA adsorbed on Au NPs are consistent with previous studies using different

nanoparticles colloids and metal substrates [23]. The broad bands at 1565 and 1341  $\text{cm}^{-1}$ , from the stretching vibrations of NH and C=N from the pt, indicate a strong and direct interaction of the nitrogen with the gold-capped silicon nanopillars. The weak interaction between the benzene ring of the paba and the Au NP is further confirmed by the presence of the Raman mode at 661  $\text{cm}^{-1}$ . The absence of bands at 1489, 1249 and 1231  $\text{cm}^{-1}$  — which are the vibration modes of the C-C, OH and O=N-C (Fig. 2(a)) from the GA fragment of the FA — suggests that the GA is not in direct contact with the Au NP. This remarkable feature leads us to conclude that the pteridine ring is probably the main part of the FA adsorbed on the surface of the Au NP.

Such changes in the SERS FA spectrum are corroborated by DFT calculations of the optimized geometry of FA molecule interacting with Au10 clusters. To decrease the high computational demands of larger clusters, an Au10 cluster has been selected and proven to be a good candidate for SERS and adsorption simulations. Our theoretical study suggests an adsorption model in which the FA interacts with the gold atoms primarily through the nitrogen atoms from the pteridine ring, as shown in Figure 4.

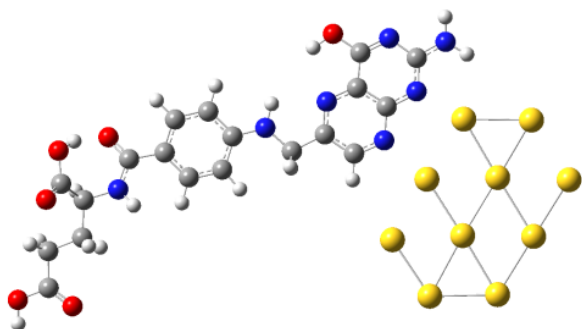


Figure 4. Optimized geometry of FA adsorbed on a cluster of 10 gold atoms

### 3.3 FA Binding to Au Surface and Adsorption Isotherm

The adsorption of FA on Au NPs was studied as a function of concentration, using the intensity of the symmetric stretching mode C=N of the pteridine ring at 689  $\text{cm}^{-1}$ . The SERS spectra of the adsorbed FA are shown in Fig. 5 (a) for seven different solution concentrations of FA, ranging between  $1 \times 10^{-9}$  and  $2 \times 10^{-3}$  M. It was observed that the maximal SERS intensity occurs at a concentration of  $0.5 \times 10^{-3}$  M (Raman band at 689  $\text{cm}^{-1}$ , Fig. 5(a)). Concentrations below  $1 \times 10^{-5}$  M exhibited a reduced Raman signal, and at concentration  $1 \times 10^{-9}$  M a weak Raman band was observed.

The intensity of the SERS band was related to the amount of FA adsorbed on the nanopillars. Therefore, to obtain more detailed information about the adsorption behaviour of FA on Au NPs, we plotted the SERS intensity versus the FA concentration. For this purpose, a SERS peak had to be selected. In the case of FA, the intensity of the symmetric stretching mode C=N of the pteridine ring at 689  $\text{cm}^{-1}$  was chosen as a marker peak.

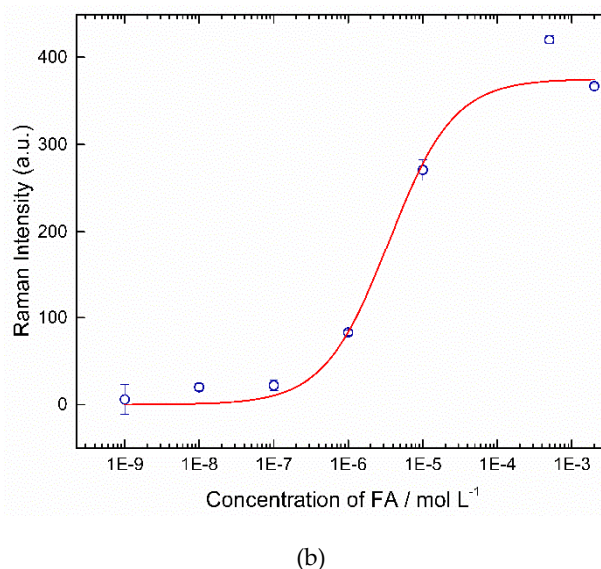
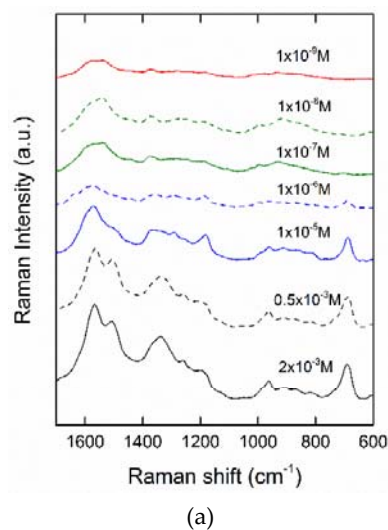


Figure 5. SERS spectra of different concentrations of FA adsorbed on gold-capped nanopillars: (a) the spectra were recorded for 5 s at a laser power of 0.1 mW; (b) SERS and adsorption isotherm of FA on Au NPs. The intensity measured at 689  $\text{cm}^{-1}$  was plotted as a function of log FA concentration.

Fig. 5(b) shows the adsorption isotherm obtained for FA at different concentrations. The equilibrium SERS intensities of FA adsorbed on silver nanopillars were fitted using nonlinear curve analysis to the Hill equation [24] of the form

$$I_{\text{SERS}} = \frac{I_{\text{max}} \times FA^n}{K_{\text{ads}} + FA^n}$$

where  $I_{\text{max}}$  is the maximal SERS intensity, FA is the concentration of the folic acid solutions,  $K_{\text{ads}}$  is the equilibrium constant for dissociation, and  $n$  is a cooperative constant.

When  $n > 1$  or  $n < 1$ , attraction and repulsion between the adsorbate molecules will take place, respectively. Note that, when  $n = 1$ , the Hill equation behaves as a Langmuir isotherm. We obtained  $K_{\text{ads}} = 4.2 \times 10^{-6} \text{ M}^{-1}$  and  $n = 0.90$ , which

indicates that the adsorption of FA to the nanopillars decreased the affinity of the new incoming FA molecules to the surface, clearly suggesting a negative cooperative binding.

Importantly, the present study, aside from offering an adsorption and the vibrational analysis study of FA on Au NPs, is a preliminary step toward the fabrication of a sensing device based on a SERS platform, in order to detect FA, or cancer cells over-expressing folate receptors at <nM concentrations.

#### 4. Conclusions

The adsorption of FA on Au NPs was carried out using SERS spectroscopy and DFT calculations. The comparison between SERS and Raman scattering spectra shows that the interaction of the FA with the Au NP surface mainly occurs through the nitrogen in the pteridine ring. This fact was further confirmed by the calculation of the optimized geometry of FA adsorbed to a cluster of 10 gold atoms. In addition, we demonstrated that FA molecules adsorbed on Au NPs follow a negative cooperative binding mechanism, from which the adsorption constant and *n*-index were calculated, being  $4.2 \times 10^{-6} \text{ M}^{-1}$  and 0.90, respectively. The present study serves as a starting point for the fabrication of a gold nanopillar-based detection system for sensing FA, or cancer cells over-expressing folate receptors.

#### 5. Acknowledgements

We are grateful for the financial support provided by the H. C. Ørsted postdoc Stipend and The Danish Council for Independent Research's NANOPLASmonic Sensors (NANOPLAS) Sapere Aude project.

#### 6. References

- [1] Castillo J J, Svendsen W E, Rozlosnik N, Escobar P, Martínez F, Castillo-León J (2012) Detection of cancer cells using a peptide nanotube-folic acid modified graphene electrode. *Analyst* 138:1026–1031.
- [2] De Bruyn E, Gulbis B, Cotton F (2014) Serum and red blood cell folate testing for folate deficiency: New features? *Eur. J. Haematol.* 92:354–359.
- [3] Ozaki Y, King R W, Carey P R (1981) Methotrexate and folate binding to dihydrofolate reductase. Separate characterization of the pteridine and p-aminobenzoyl binding sites by resonance Raman spectroscopy. *Biochemistry* 20:3219–3225.
- [4] Liu L, Zhu X, Zhang D, Huang J, Li G (2007) An electrochemical method to detect folate receptor positive tumor cells. *Electrochem. commun.* 9:2547–2550.
- [5] Izquierdo-Lorenzo I, Sanchez-Cortes S, Garcia-Ramos J V (2011) Trace detection of aminoglutethimide drug by surface-enhanced Raman spectroscopy: a vibrational and adsorption study on gold nanoparticles. *Anal. Methods* 3:1540.
- [6] Wu Q, Luo C, Yu H, Kong G, Hu J (2014) Surface sol-gel growth of ultrathin SiO<sub>2</sub> films on roughened Au electrodes: Extending borrowed SERS to a SERS inactive material. *Chem. Phys. Lett.* 608:35–39.
- [7] Jarvis R M, Johnson H E, Olembe E, Panneerselvam A, Malik Ma, Afzaal M, O'Brien P, Goodacre R (2008) Towards quantitatively reproducible substrates for SERS. *Analyst* 133:1449–1452.
- [8] Schmidt M S, Hübner J, Boisen A (2012) Large area fabrication of leaning silicon nanopillars for Surface Enhanced Raman Spectroscopy. *Adv. Mater.* 24:1–8.
- [9] Yang J, Palla M, Bosco FG, Rindzevicius T, Alstrøm T S, Schmidt M S, Boisen A, Ju J, Lin Q (2013) Surface-enhanced Raman spectroscopy based quantitative bioassay on aptamer-functionalized nanopillars using large-area Raman mapping. *ACS Nano* 7:5350–5359.
- [10] Dong O, Lam D C C (2011) Silver nanoparticles as surface-enhanced Raman substrate for quantitative identification of label-free proteins. *Mater. Chem. Phys.* 126:91–96.
- [11] Jing C, Fang Y (2007) Experimental (SERS) and theoretical (DFT) studies on the adsorption behaviors of L-cysteine on gold/silver nanoparticles. *Chem. Phys.* 332:27–32.
- [12] Muniz-Miranda M, Gellini C, Pagliai M, Innocenti M, Salvi P R, Schettino V (2010) SERS and computational studies on microRNA chains adsorbed on silver surfaces. *J. Phys. Chem. C.* 114:13730–13735.
- [13] Liu R, Zhang D, Cai C, Xiong Y, Li S, Su Y, Si M (2013) NIR-SERS studies of DNA and DNA bases attached on polyvinyl alcohol (PVA) protected silver grass-like nanostructures. *Vib. Spectrosc.* 67:71–79.
- [14] Boca-Farcau S, Potara M, Simon T, Juhem A, Baldeck P, Astilean S (2014) Folic acid-conjugated, SERS-labeled silver nanotriangles for multimodal detection and targeted photothermal treatment on human ovarian cancer cells. *Mol. Pharm.* 11:391–399.
- [15] Hu C, Liu Y, Qin J, Nie G, Lei B, Xiao Y, Zheng M, Rong J (2013) Fabrication of reduced graphene oxide and silver nanoparticle hybrids for Raman detection of absorbed folic acid: A potential cancer diagnostic probe. *ACS Appl. Mater. Interfaces* 5:4760–4768.
- [16] Kokaislová A, Helešicová T, Ončák M, Matějka P (2014) Spectroscopic studies of folic acid adsorbed on various metal substrates: does the type of substrate play an essential role in temperature dependence of spectral features? *J. Raman. Spectrosc.* 45:750–757.

- [17] Castillo J, Bertel L, Páez-Mozo E, Martínez F (2013) Photochemical Synthesis of the Bioconjugate Folic Acid-Gold Nanoparticles. *Nanomater. Nanotechnol.* 3:1.
- [18] Scott A P, Radom L (1996) Harmonic Vibrational Frequencies: An Evaluation of Hartree-Fock, Møller-Plesset, Quadratic Configuration Interaction, Density Functional Theory, and Semiempirical Scale Factors. *J. Phys. Chem.* 100(d):16502–16513.
- [19] Zhang L, Fang Y, Zhang P (2008) Experimental and DFT theoretical studies of SERS effect on gold nanowires array. *Chemical Physics Letters* 102–105.
- [20] Sakata K, Tada K, Yamada S, Kitagawa Y, Kawakami T, Yamanaka S, Okumura M (2013) DFT calculations for aerobic oxidation of alcohols over neutral Au<sub>6</sub> cluster. *Mol. Phys.* 112:385–392.
- [21] Wadt W R, Hay P J (1985) Ab initio effective core potentials for molecular calculations. Potentials for main group elements Na to Bi. *J. Chem. Phys.* 82(May 2014):284–298.
- [22] Joo S W, Han S W, Kim K (2001) Adsorption of 1,4-Benzenedithiol on Gold and Silver Surfaces: Surface-Enhanced Raman Scattering Study. *J. Colloid. Interface Sci.* 240:391–399.
- [23] Goh D, Dinish U S, Olivo M (2012) Optimized Bi-Metallic Film over Nanosphere SERS Substrate for Sensitive Detection of Folic Acid. *Photonics Global Conference (PGC)* 2–5.
- [24] Weiss J N (1997) The Hill equation revisited: uses and misuses. *FASEB J* 11:835–841.